Molecular Vision 2021; 27:107-116 <http://www.molvis.org/molvis/v27/107>
Received 29 July 2020 | Accepted 16 March 2021 | Published 18 March 2021

Heterozygous deletions of noncoding parts of the *PRPF31* gene cause retinitis pigmentosa via reduced gene expression

Francesco Paolo Ruberto,[1] Sara Balzano,[2] Prasanthi Namburi,[3] Adva Kimchi,[3] Rosanna Pescini-Gobert,[2] Alexey Obolensky,[3] Eyal Banin,[3] Tamar Ben-Yosef,[4] Dror Sharon,[3] Carlo Rivolta[5,6,7]

(The first three authors contributed equally to this study.)

[1]Experimental Cardiology Unit, Department of Cardiovascular Medicine, University of Lausanne Medical School, Lausanne, Switzerland; [2]Department of Computational Biology, University of Lausanne, Lausanne, Switzerland; [3]Department of Ophthalmology, Hadassah Medical Center, Faculty of Medicine, The Hebrew University of Jerusalem, Jerusalem, Israel; [4]Rappaport Faculty of Medicine, Technion- Israel Institute of Technology, Haifa, Israel; [5]Institute of Molecular and Clinical Ophthalmology Basel (IOB), Basel, Switzerland; [6]Department of Ophthalmology, University of Basel, Basel, Switzerland; [7]Department of Genetics and Genome Biology, University of Leicester, Leicester, United Kingdom

Purpose: Heterozygous mutations in the gene *PRPF31*, encoding a pre-mRNA splicing factor, cause autosomal dominant retinitis pigmentosa (adRP) with reduced penetrance. At the molecular level, pathogenicity results from haploinsufficiency, as the largest majority of such mutations trigger nonsense-mediated mRNA decay or involve large deletions of coding exons. We investigated genetically two families with a history of adRP, one of whom showed incomplete penetrance.
Methods: All patients underwent thorough ophthalmological examination, including electroretinography (ERG) and Goldmann perimetry. Array-based comparative genomic hybridization (aCGH) and multiplex ligation-dependent probe amplification (MLPA) were used to map heterozygous deletions, while real-time PCR on genomic DNA and long-range PCR allowed resolving the mutations at the base-pair level. *PRPF31* transcripts were quantified with real-time PCR on patient-derived lymphoblastoid cell lines.
Results: We identified two independent deletions affecting the promoter and the 5′ untranslated region (UTR) of *PRPF31* but leaving its coding sequence completely unaltered. Analysis of *PRPF31* mRNA from lymphoblastoid cell lines from one of these families showed reduced levels of expression in patients versus controls, probably due to the heterozygous ablation of its promoter sequences.
Conclusions: In addition to reporting the identification of two novel noncoding deletions in *PRPF31*, this study provides strong additional evidence that mRNA-mediated haploinsufficiency is the primary cause of pathogenesis for *PRPF31*-linked adRP.

Retinitis pigmentosa (RP) is the most common form of inherited retinal dystrophy, a class of diseases characterized by progressive degeneration of photoreceptors, the light-sensing cells of the human retina [1]. This condition affects approximately 1 in 3,500 individuals worldwide [2] and is usually inherited as a monogenic trait (dominant, recessive, or X-linked), despite being very heterogeneous at the genetic level [3].

PRPF31 is a ubiquitous pre-mRNA splicing factor, which is part of the U4/U6*U5 trimeric small nuclear ribonucleoprotein complex of the spliceosome, is essential for cell survival, and is highly conserved within all eukaryotes, from yeast to humans. In humans, PRPF31 is encoded by the *PRPF31* (Gene ID: 26121; OMIM: 606419) gene, localized at chromosome 19q13.4 and constituted by 14 exons in its main mature isoform.

Despite the observation that complete *PRPF31* deficiency is not compatible with life [4], heterozygous mutations of various types (nonsense, missense, and frameshift) are associated with nonsyndromic autosomal dominant retinitis pigmentosa (adRP) [5]. The majority of the reported mutations result in premature stop codons leading to nonsense-mediated mRNA decay (NMD) of mutated transcripts, and therefore, to disease by haploinsufficiency [6]. The link between defects in such a fundamental gene and a tissue-restricted phenotype such as RP has not been fully elucidated.

PRPF31-associated RP displays sometimes incomplete penetrance, which is, in fact, a clinical hallmark of the involvement of this gene in the pathology. That is, carriers of heterozygous mutations in *PRPF31* may or may not develop the disease throughout their life, and therefore, either be affected by progressive blindness or else be completely asymptomatic (while, however, still being able to pass

Correspondence to: Carlo Rivolta, Institute of Molecular and Clinical Ophthalmology Basel (IOB), Mittlere Strasse 91, CH-4031 Basel, Switzerland; Phone: +41 61 568 7211; FAX: +41 61 265 8652; email: carlo.rivolta@iob.ch

pathogenic mutations to their offspring) [7,8]. This differential phenotype seems to depend, in turn, on the differential expression of the *PRPF31* allele that does not bear the mutation. High expressors compensate for the protein deficiency induced by NMD on the mutated allele and have normal vision, whereas low expressors suffer from retinal degeneration due to an inadequate amount of functional PRPF31 protein [9,10]. The 5′ untranslated region (UTR) of the gene *TCF3 fusion partner* (*TFPT;* Gene ID: 29844; OMIM 609519) overlaps with that of *PRPF31*; the two genes are arranged in a "head-to-head" configuration and are transcribed from opposite DNA strands. TFPT has not been fully characterized, but its protein product has been identified as a molecular partner of transcription factor 3 (TCF3 or E2A) in childhood leukemia, and seems to function as a proapoptotic factor, putatively involved in cerebral apoptosis [11]. It has also been hypothesized that *PRPF31* and *TFPT* share the same bidirectional promoter, and that expression of the two genes is coregulated [12,13]. Furthermore, the genomic region comprising *TFPT* and *PRPF31* is characterized by the presence of multiple repetitive Alu elements in intergenic and intragenic sequences, putatively promoting recombination events, such as deletions, duplications, and copy number variations in general [14].

In this article, we report the identification of two noncoding deletions spanning *PRPF31* and *TFPT* core promoters as well as *PRPF31*'s 5′ UTR, in two families with adRP (one non-penetrant). This work shows that, in addition to mutations affecting *PRPF31*'s open reading frame, disease can be triggered by promoter-induced hypoexpression of the non-mutated *PRPF31* coding sequence, presumably according to the same mechanisms of haploinsufficiency that are typical of all NMD-inducing mutations in *PRPF31* detected thus far.

METHODS

Patients and clinical evaluation: We studied two unrelated families of Ashkenazi Jewish descent (MOL0931 and TB228) with a history of adRP. All participating individuals signed a consent form, in agreement with the Declaration of Helsinki and the ARVO statement on human subjects. The study was approved by the institutional review boards of our respective institutions. Ocular evaluation included measurement of best-corrected visual acuity (BCVA), fundus examination after pupillary dilatation, fundus photography, spectral-domain optical coherence tomography (SD-OCT), full-field electroretinogram (ffERG), and visual field testing.

Cell cultures and immortalization: Peripheral blood mononuclear cells (PBMCs) were collected from the five members of the family MOL0931, and lymphocytes were immortalized from peripheral blood using the Epstein-Barr virus, to produce lymphoblastoid cell lines (LCLs). They were grown in Roswell Park Memorial Institute (RPMI) 1640 (Gibco, Waltham, MA) supplemented with 10% fetal bovine serum (FBS) and 1% penicillin-streptomycin, as described in the literature [15].

DNA and RNA extraction, cDNA synthesis: Total genomic DNA was purified from peripheral blood leukocytes using the illustra Nucleon BACC genomic DNA extraction kit (GE Lifescience, Chicago, IL). RNA was extracted from the LCLs using the RNeasy mini kit (Qiagen, Hilden, Germany), according to the manufacturer's instructions. Total RNA was then retrotranscribed using oligo dT and random hexamers in combination with the GoScript™ Reverse Transcription System (Promega, Madison, WI), as reported in the manufacturer's protocol. Control RNA was extracted and retrotranscribed to cDNA from 13 LCL samples derived to the CEPH reference panel [16], according to the same conditions.

Array CGH and MLPA: Genomic DNA samples of MOL0931–1 and MOL0931–2 were tested with array-based comparative genomic hybridization (aCGH) targeted for *PRPF31* at GeneDx (Gaithersburg, MD). The array contains DNA oligonucleotide probes in or flanking *PRPF31* exons. The array is designed to detect most single-exon deletions and duplications. Data analysis was performed with the Agilent Genomic Workbench software (Santa Clara, CA), with gene-specific filtering with the Cartagenia BENCH software (Agilent). Fragment analysis multiplex ligation-dependent probe amplification (MLPA) of the *PRPF31* gene in individual TB228-1 was performed using the SALSA MLPA Probemix P235-B3 (MRC-Holland, Amsterdam, the Netherlands), according to the manufacturer's instructions.

PRPF31 expression analysis with real-time PCR: Real-time PCR was performed using the SYBR Green PCR Master Mix (Applied Biosystems, Foster City, CA). We used three identical replicates for each real-time experiment. *GAPDH* (Gene ID: 2597 ; OMIM: 138400) and human beta actin (*ACTB*; Gene ID: 60; OMIM: 102630) cDNA derived from mRNA was used to normalize *PRPF31* mRNA expression during quantification.

To confirm the absence of genomic DNA in cDNA preparations, control reactions lacking the reverse transcriptase enzyme (−RT) were performed. These preparations were run in parallel and used as negative controls for each RT–PCR.

Real-time PCR on genomic DNA, long-range PCR, and DNA sequencing: Primers for quantitative amplification of genomic DNA in family MOL0931 are listed in Supplementary Table 1. The primers were designed to match unique

genomic regions using Primer 3 plus, and the in silico amplification product was tested using the UCSC in-Silico PCR tool. Assessment of hemizygous genotypes in the carriers of mutations in *PRPF31* and in men versus women, for the *XIST* (Gene ID: 7503; OMIM: 314670) gene, was performed as described previously [17]. In short, the readouts of these amplifications were standardized by measuring the signals produced by a portion of *XIST* and then normalized to signals from a bona fide diploid portion of *PRPF31*, located on exon 8 (primers 5′-CCT GAC CAA CCT CTC CAA GA-3′, 5′-GTA GAC GAG AAG CCC GAC AG-3′). The ratio between the threshold cycle (Ct) values of regions to be investigated for the copy number and the Ct value of exon 8 gave us an indication of the mono- or biallelic genetic content.

The long-range PCR encompassing exon 3 of *TFPT* and the intronic proximities of exon 2 of *PRPF31* was achieved with use of the high-fidelity Phusion DNA polymerase (TaKaRa, Shiga, Japan), primers 5′-GGA TGT GGA AGT GGG AGA GA-3′ (forward) and 5′-GGC GAT GGT CTT GAC TGA AT-3′ (reverse), and a "touchdown" cycling profile. In essence, following an initial denaturation step at 98 °C for 3 min, the samples were subjected to the following conditions: 15 cycles at 98 °C for 10 s + 66 °C (decreasing by 0.7 °C per cycle) for 30 s+ 72 °C for 9 min, followed by 25 cycles at 98 °C for 10 s + 55 °C for 30 s + 72 °C for 9 min. The amplification buffer (20 µl) was composed of Phusion Buffer, 4 µl; 10 mM deoxynucleotide triphosphate (dNTPs), 0.4 µl; forward primer 10 µM, 1 µl; reverse primer 10 µM, 1 µl; 10 ng/µl DNA, 10 µl; dimethyl sulfoxide (DMSO), 0.6 µl; Phusion polymerase, 0.2 µl; and H_2O, 2.8 µl. All the amplification products from patients and controls were sequenced with the Sanger method by using 16 different primers spanning the entire fragment (Supplementary Table 2). Standard PCRs to confirm the deletion breakpoints were performed with the use of the GoTaq polymerase (Promega), a standard amplification buffer, the cycling conditions 94 °C for 3 min, [94 °C for 30 s + 60 °C for 30 s+ 72 °C for 30 s] for 30 cycles, and 72 °C for 3 min, and the primers listed in Supplementary Table 3.

In silico analyses: Basic bioinformatics analyses were performed with tools from the University of California Santa Cruz (USCS) Genome Browser, including RepeatMasker, for the detection of Alu elements and other repetitive sequences within the *PRPF31* locus.

RESULTS

Clinical findings: Family MOL0931 of Ashkenazi Jewish origin included three individuals affected with RP: the index case (MOL0931–1), his sister (MOL0931–2), and his paternal grandmother (MOL0931–5). The proband's father had no symptoms, suggesting dominant inheritance with incomplete penetrance (Figure 1). The index case was noted to have impaired night vision at age 11, but only at age 17 was the diagnosis of RP established, based on funduscopic findings and non-detectable electroretinogram (ERG) responses under all stimulus conditions. His VA was 20/25 in the right eye and 20/30 in the left eye. Intraocular pressure (IOP) was within normal limits, and anterior segments were quiet and clear with no evidence of cataracts. There were strands and floaters in the vitreous as well as +1 cells. Funduscopic findings were those characteristic of RP, including pallor of the optic discs, attenuated retinal vessels, and widespread grayish spots of atrophy, as well as bone spicule-like pigmentation throughout the retina, with somewhat better preservation of retinal color in the macular area. There were cystoid macular changes and mild epiretinal membranes. One year later, at age 18, VA was 20/40 in both eyes, and the cystoid changes had worsened considerably. Oral administration of acetazolamide 125 mg three times daily yielded significant reduction in the degree of macular edema (Figure 2A–D). Goldmann visual fields at age 18 were constricted to 10–15 degrees from fixation using the V4e target, and there were preserved islands of vision in the far temporal periphery of both eyes (Figure 2E,F). His sister, at age 15, had much better fields, with mild to moderate superior and nasal constriction but well-preserved temporal fields with the V4e target (Figure 2G,H). OCT performed at the age of 22 showed preservation of the outer nuclear layer (ONL) and the ellipsoid zone (EZ) in the foveal region, but marked thinning of the ONL and loss of the EZ outside this area (Figure 2I,J). The father of the two siblings (MOL0931–3) was asymptomatic. His VA was 20/20 in both eyes, and his clinical ophthalmological exam was within normal limits without funduscopic signs of retinal degeneration. ffERG testing performed at the age of 51 years showed normal dark-adapted rod b-wave responses and normal light-adapted cone responses, including normal cone flicker implicit times. The dark-adapted mixed rod-cone response to an International Society for Clinical Electrophysiology of Vision (ISCEV) standard flash showed normal amplitude of the a-wave, while the b-wave was reduced to approximately 70% of the lower limit of normal (Table 1).

The second family (TB228) is an Ashkenazi Jewish family, segregating adRP with no indication for reduced penetrance (Figure 1). The index patient (TB228–1) was diagnosed with RP at the age of 47 years. At this age, his scotopic and photopic ffERG recordings were severely reduced. He reported that his father and his brother had RP, but no clinical data were available. He has two sons. One (TB228–3) had normal vision. The second son (TB228–2)

had night blindness since childhood and was diagnosed with RP at the age of 8 years. At the age of 11 years, his scotopic and photopic ERG recordings were severely reduced, and by the age of 17 years, his ffERG was nonrecordable. At the age of 38 years, he underwent cataract surgery in his left eye. A year later, OCT imaging demonstrated thinning of the retina with flattening of the foveal depression in both eyes and an epiretinal membrane in the left eye. At the age of 43 years, he had severe constriction of the visual field. At this time, his BCVA was 20/20 (right eye) and 20/100 (left eye). Funduscopy revealed extensive retinal pigment deposits and optic disc pallor on both eyes. Summary clinical findings are reported in Table 1.

Molecular genetics: For family MOL0931, genetic analysis for the two affected siblings including screening of previously reported mutations using the Asper mutation detection array and Sanger sequencing of candidate exons was negative. Whole exome sequencing (WES) analysis was subsequently performed on DNA samples of the three affected individuals but did not reveal any potential pathogenic variants. Array CGH analysis of the two affected siblings allowed identification of a putative heterozygous deletion involving exon 1 of *PRPF31*, which is noncoding, and possibly other regions of the same gene.

For family TB228, TB228–1 and TB228–2 underwent whole exome sequencing, with negative results. Fragment analysis MLPA of the *PRPF31* gene in individual TB228–1 indicated a putative heterozygous deletion involving exon 1 of *PRPF31.*

Prompted by the array CGH (family MOL0931) and MLPA (family TB228) data, we hypothesized and investigated the presence of a large heterozygous deletion, which is a common cause of pathogenesis in *PRPF31*-associated RP [14]. To this end, we designed a series of very-short range (maximum 143 bp) real-time PCRs by using as a template the genomic DNA from the three patients and the asymptomatic obligated carrier from family MOL0931, as well as from four control subjects.

Of the 12 PCRs performed, four PCRs were compatible with the hemizygous presence of template DNA (Figure 3). Interestingly, these amplifications were all contiguous and flanked on both sides by PCRs outputting results from diploid DNA, in agreement with the presence of a putative heterozygous deletion within the *PRPF31* gene. Specifically,

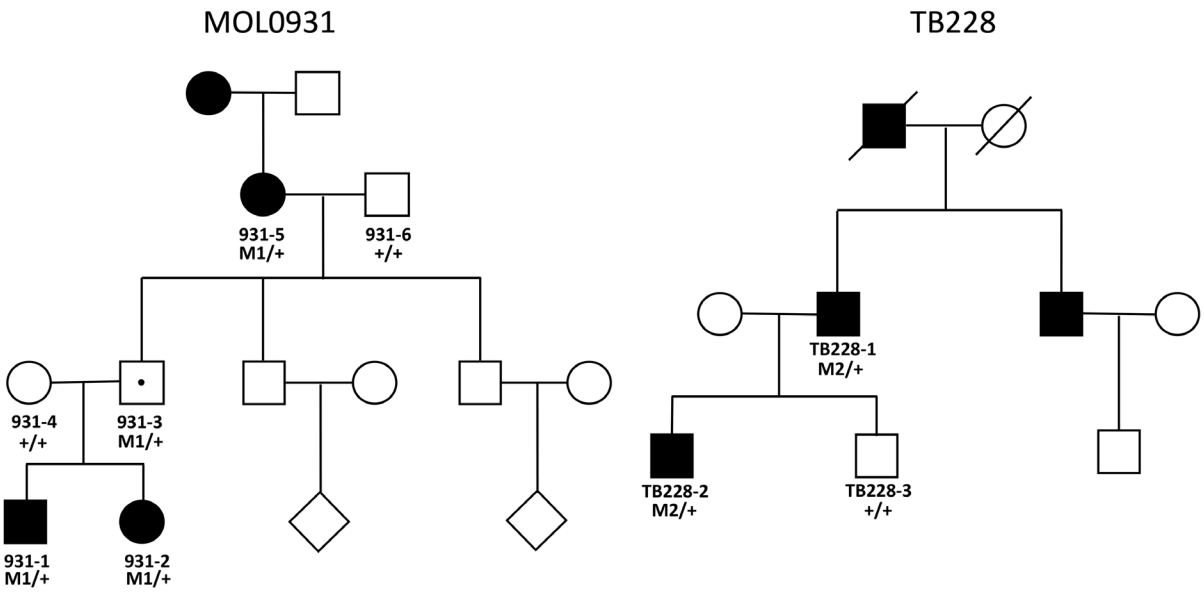

Figure 1. Structure of the pedigrees investigated in this study. Open symbols represent unaffected individuals (squares: males, circles: females), whereas filled symbols indicate patients. The central dot indicates the status of an unaffected carrier of mutation. +, wild-type allele; M1, chr19: g.54113356-54116922del; M2, g.54113882-54116394del.

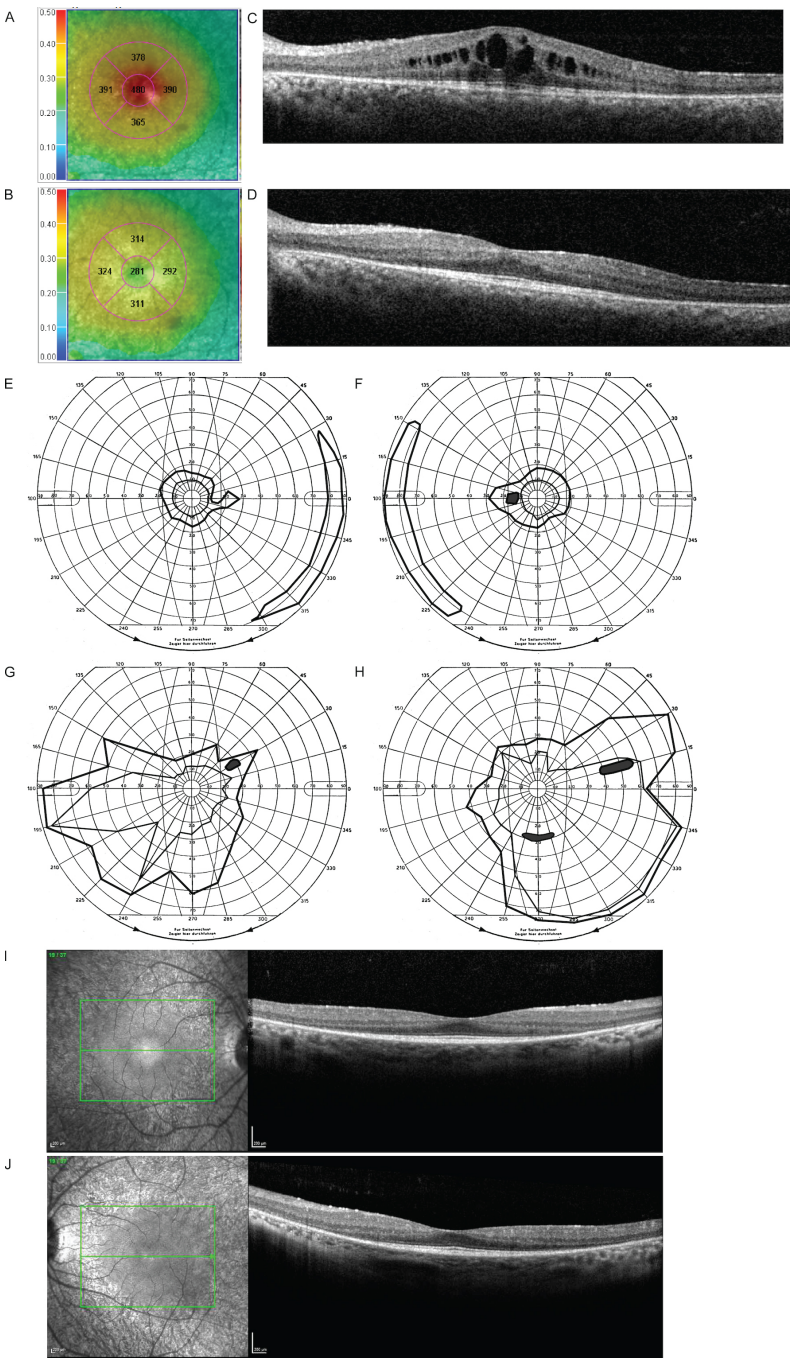

Figure 2. Imaging of patients MOL0931–1 and MOL0931–2. **A**–**D**: Optical coherence tomography (OCT) map and representative macular scans of MOL0931–1 at the age of 18 years, before treatment (**A**,**C**) and following treatment with 125 mg acetazolamide three times daily (**B**,**D**). **E**–**H**: Goldmann visual fields of MOL0931–1 at age 18 (**E**,**F**) and his sister MOL0931–2 at age 15 (**G**,**H**). **I**–**J**: OCT scans of MOL0931–2 at age 22.

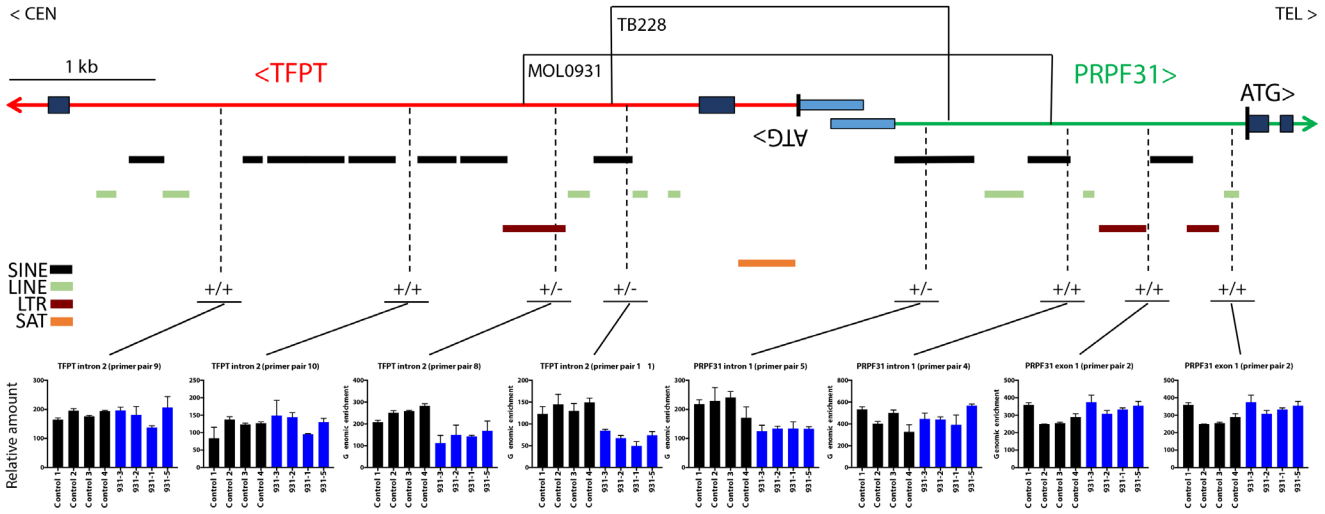

Figure 3. Schematic representation of the *PRPF31* region and of the deletions identified. The structure of the *PRPF31* (green) and *TFPT* (red) genes is indicated (introns, lines; noncoding exons, light-blue boxes; coding exons, dark blue boxes). The deletions detected in families MOL0931 and TB228 are indicated by the black lines. Repeated DNA elements are indicated by boxes in color (SINE, short interspersed nuclear elements; LINE, long interspersed nuclear elements; LTR, long-terminal repeats; SAT, microsatellites). Results of real-time PCRs on the genomic DNA from members of the MOL0931 family are shown by the graphs at the bottom, indicating the presence of two DNA copies (+/+) or one DNA copy of the region investigated (+/−). Because of space constraints, only eight primer pairs of the 12 used are depicted in this image. TEL, telomere; CEN, centromere.

the last positive diploid amplifications were in intron 2 of *TFPT* and intron 1 of *PRPF31*, from the centromeric and telomeric ends, respectively, indicating that such deletion could include exons 1 and 2 of *TFPT* and exon 1 of *PRPF31*. Therefore, we set up a long-range PCR (8.3 kb) that could span the breakpoint of the deletion, by anchoring primers on exon 3 of *TFPT* and a portion of intron 1 of *PRPF31* neighboring exon 2, that is, the closest regions devoid of repetitive DNA elements (Figure 4A). Sequencing of this amplification product identified the breakpoint of a 3,567 bp deletion (hg38; chr19: g.54113356-54116922del), originating in intron 2 of *TFPT* and ending in intron 1 of *PRPF31*, likely as a consequence of an Alu-mediated recombination (Figure 3, Figure 5). This event was further validated with a short-range "diagnostic" PCR performed directly on the genome of patients and controls, with primers located immediately across the breakpoint (Supplementary Table 3, Figure 4B) and with Sanger sequencing of the PCR product. In these tests, only DNAs from patients result in a signal, as the distance between the forward and reverse primers in the absence of the deletion would be too large to yield any PCR product in standard conditions (Figure 4A,B).

Table 1. Clinical characteristics of the individuals ascertained.

Diagnosis	ERG			Visual acuity (right eye, left eye)	Age at exam (years)	Sex	Individual ID
	30 Hz cone flicker	Mixed cone-rod response	Rod response				
RP	NR	NR	NR	6/9, 6/7.5	17	M	MOL0931–1
RP					15	F	MOL0931–2
Unaffected carrier	WNL	a-wave: WNL b-wave: 70%*	WNL	6/6, 6/6	51	M	MOL0931–3
RP	ND	NR	Severely reduced	N/A	47	M	TB228–1
RP	ND	NR	NR	6/6, 6/30	41	M	TB228–2

NR: non-recordable; ND: not done; WNL- within normal limits *- 70% of lower limit of normal.

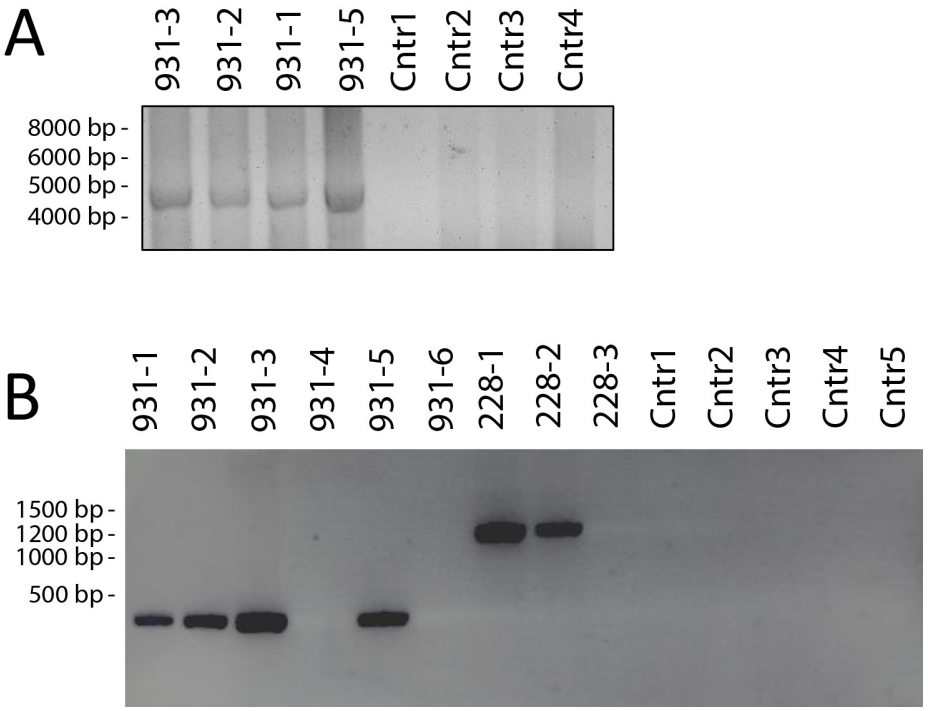

Figure 4. Long- and short-range PCRs spanning the two mutations. **A**: Long-range PCR on DNA from members of family MOL0931 and four controls. Only deletion-carrying alleles output a PCR product, as for wild-type alleles the distance between the primers used is too long to result in any amplification. **B**: "Diagnostic" short-range PCR in members of both families, as well as five control individuals. The rationale for the presence or absence of a PCR product is the same as that explained for panel **A**.

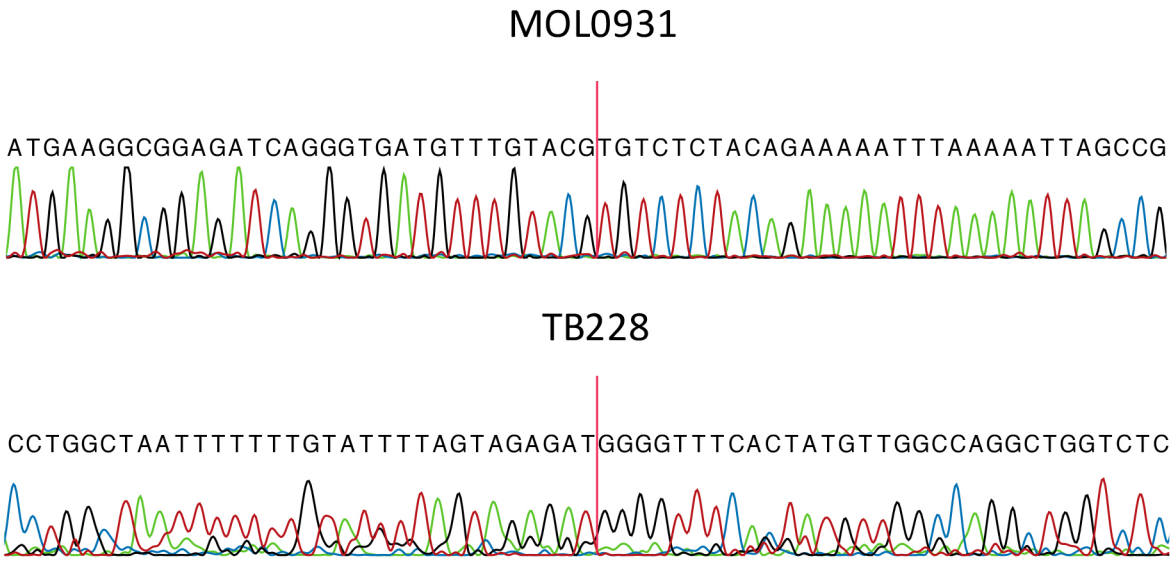

Figure 5. Sequences of the breakpoints. Electropherograms of the breakpoints of the two deletions. The red lines indicate the junction between DNA originating from intron 2 of *TFPT* (on the left) and DNA originating from intron 1 of *PRPF31* (right).

PCR analysis and Sanger sequencing on DNA from family TB228 revealed a shorter deletion (g.54113882-54116394del; 2,513 bp) at the same locus in affected individuals TB228–1 and TB228–2. This event, which removed the same exons that were ablated in patients from family MOL0931, was not present in unaffected individual TB228–3 (Figure 4B). The deletion's boundaries included intron 2 of *TFPT* and intron 1 of *PRPF31*, within the vicinity of two short interspersed nuclear elements (SINE) repetitive elements (Figure 3, Figure 5).

Expression analyses: Molecular pathogenesis of mutations in *PRPF31* is almost invariably associated with DNA variants that lead to reduced expression of the allele that carries the mutation, via a mechanism of haploinsufficiency [9,10]. In most cases, this is the consequence of mutations leading to premature termination triplets in the coding sequence and therefore, to nonsense-mediated mRNA decay of the transcript [6]. However, in at least one instance reported in the literature the same pathological effect is produced by a single-base mutation in the promoter, leading to hypoexpression of wild-type *PRPF31* mRNA [12]. To test whether the deletions identified in this study, involving noncoding parts of the gene and encompassing its promoter, could induce pathogenesis by the same mechanism, we assessed *PRPF31* expression in LCLs from the four carriers of mutations from family MOL0931 and compared it to that of LCLs from 13 controls, according to well-established protocols for this specific analysis [9,10,17]. Fresh biological material from family TB228 was unavailable, and therefore, this test could not be performed on members from this pedigree.

In agreement with previous literature testing coding mutations in *PRPF31*, individuals carrying the noncoding chr19: g.54113356-54116922del mutation had markedly reduced levels of *PRPF31* transcripts compared to controls, whereas MOL0931–3 had intermediate amounts of mRNA, slightly higher than those of patients (Figure 6).

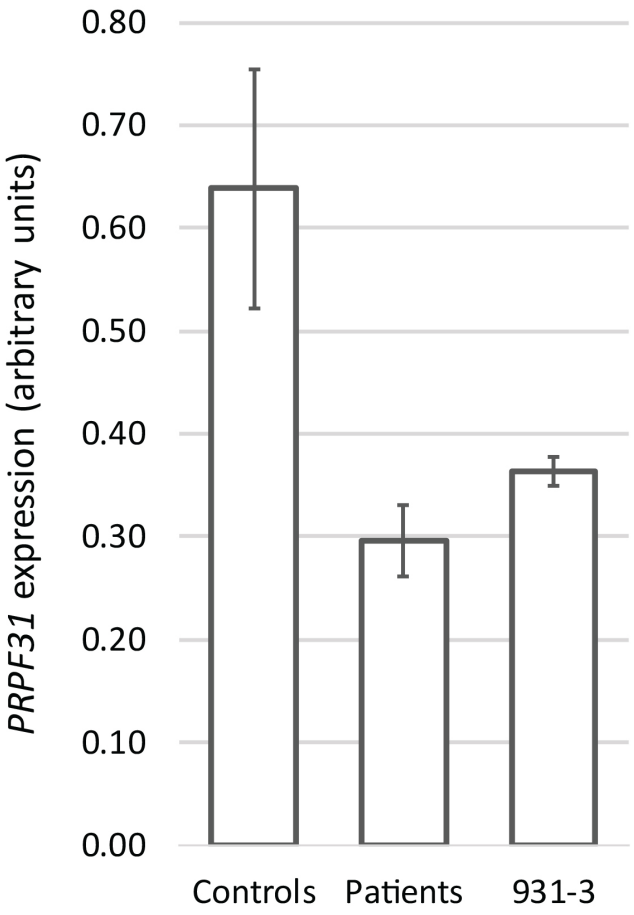

Figure 6. Real-time PCR from lymphoblastoid cell lines from family MOL0931 and from controls. Relative *PRPF31* expression in 13 controls, patients from family MOL0931 (931–1, 931–2, and 931–5), and individual 931–3 (unaffected carrier of the mutation) are shown. Error bars indicate standard deviations. The difference in gene expression between controls and patients is statistically significant ($p = 1.3 \times 10^{-4}$, by *t* test).

DISCUSSION

In adRP associated with mutations in *PRPF31*, pathogenicity is prevalently triggered by hemizygosity of its transcripts (haploinsufficiency). This, in turn, is due to three main causes: single-base or small mutations leading to premature termination codons and therefore, to NMD (most cases) [6], large deletions involving one or several coding exons [14,18,19], or heterozygous mutations in regulatory regions. To the best of our knowledge, there is only one example of the latter mechanism, involving a single base deletion in the 5′ UTR of *PRPF31* [12].

In this work, we report the identification of two deletions spanning exon 1 (noncoding) of *PRPF31*, as well as its core promoter. In contrast to the largest majority of mutations detected thus far, both mutations reported here leave *PRPF31*'s open reading frame untouched. However, similar to all other mutations investigated thus far, these deletions also result in a reduction in *PRPF31* transcripts, and therefore, presumably in a pathogenic mechanism related to haploinsufficiency of the PRPF31 protein. In the present case, however, the reduction in *PRPF31* expression should not be triggered by NMD, but by ablation of the gene's promoter sequences, as defined by Rose et al. [12]. The levels of *PRPF31* mRNA expression displayed by cell lines from individual MOL0931–3, having an intermediate value between patients and controls, are also

typical, although they are not really predictive of his present or future clinical status [9,10].

It is also remarkable that two mutational events within the same genomic interval, of similar nature, and resulting in the same phenotype were of independent origin. This is even more striking if we consider that the two families in which the deletions occurred were from the same ethnic group, and therefore, we would have expected the presence of an ancestral mutation, common to both pedigrees. A likely explanation for these findings is that the presence of multiple repetitive DNA elements in this region makes it particularly unstable and prone to events of uneven recombination, resulting in turn in deletions or duplications. In summary, in addition to reporting the identification of two novel noncoding mutations in *PRPF31*, these results provide an additional element of support for the notion that retinal pathogenesis is due to the gene's hypoexpression, rather than to the mere presence of mutations in the gene's coding sequence.

APPENDIX 1. SUPPLEMENTARY TABLE 1.

Primers used for qPCR on genomic DNA. To access the data, click or select the words "Appendix 1."

APPENDIX 2. SUPPLEMENTARY TABLE 2.

Sequencing primers for long-range PCR product. To access the data, click or select the words "Appendix 2."

APPENDIX 3. SUPPLEMENTARY TABLE 3.

Primers for diagnostic PCR. To access the data, click or select the words "Appendix 3."

ACKNOWLEDGMENTS

This work was supported by a grant from the Swiss National Science Foundation (grant 31003A_176097, to CR) and a grant from the Foundation Fighting Blindness USA (BR-GE-0214–0639-TECH to TB, DS, and EB). The authors thank Devora Marks-Ohana for technical assistance and Sitta Föhr for her help with the copyediting of the manuscript. We warmly thank all patients and their family members for participating in this study.

REFERENCES

1. Berson EL. Retinitis pigmentosa. The Friedenwald Lecture. Invest Ophthalmol Vis Sci 1993; 34:1659-76. [PMID: 8473105].
2. Hanany M, Rivolta C, Sharon D. Worldwide carrier frequency and genetic prevalence of autosomal recessive inherited retinal diseases. Proc Natl Acad Sci USA 2020; 117:2710-6. [PMID: 31964843].
3. Rivolta C, Sharon D, DeAngelis MM, Dryja TP. Retinitis pigmentosa and allied diseases: numerous diseases, genes, and inheritance patterns. Hum Mol Genet 2002; 11:1219-27. [PMID: 12015282].
4. Weidenhammer EM, Singh M, Ruiz-Noriega M, Woolford JL. The PRP31 gene encodes a novel protein required for pre-mRNA splicing in Saccharomyces cerevisiae. Nucleic Acids Res 1996; 24:1164-70. [PMID: 8604353].
5. Vithana EN, Abu-Safieh L, Allen MJ, Carey A, Papaioannou M, Chakarova C, Al Maghtheh M, Ebenezer ND, Willis C, Moore AT, Bird AC, Hunt DM, Bhattacharya SS. A human homolog of yeast pre-mRNA splicing gene, PRP31, underlies autosomal dominant retinitis pigmentosa on chromosome 19q13.4 (RP11). Mol Cell 2001; 8:375-81. [PMID: 11545739].
6. Rio Frio T, Wade NM, Ransijn A, Berson EL, Beckmann JS, Rivolta C. Premature termination codons in PRPF31 cause retinitis pigmentosa via haploinsufficiency due to nonsense-mediated mRNA decay. J Clin Invest 2008; 118:1519-31. [PMID: 18317597].
7. Berson EL, Gouras P, Gunkel RD, Myrianthopoulos NC. Dominant retinitis pigmentosa with reduced penetrance. Arch Ophthalmol 1969; 81:226-34. [PMID: 5764686].
8. Kiser K, Webb-Jones KD, Bowne SJ, Sullivan LS, Daiger SP, Birch DG. Time Course of Disease Progression of PRPF31-mediated Retinitis Pigmentosa. Am J Ophthalmol 2019; 200:76-84. [PMID: 30582903].
9. Rivolta C, McGee TL, Rio Frio T, Jensen RV, Berson EL, Dryja TP. Variation in retinitis pigmentosa-11 (PRPF31 or RP11) gene expression between symptomatic and asymptomatic patients with dominant RP11 mutations. Hum Mutat 2006; 27:644-53. [PMID: 16708387].
10. Vithana EN, Abu-Safieh L, Pelosini L, Winchester E, Hornan D, Bird AC, Hunt DM, Bustin SA, Bhattacharya SS. Expression of PRPF31 mRNA in patients with autosomal dominant retinitis pigmentosa: a molecular clue for incomplete penetrance? Invest Ophthalmol Vis Sci 2003; 44:4204-9. [PMID: 14507862].
11. Franchini C, Fontana F, Minuzzo M, Babbio F, Privitera E. Apoptosis promoted by up-regulation of TFPT (TCF3 fusion partner) appears p53 independent, cell type restricted and cell density influenced. Apoptosis 2006; 11:2217-24. [PMID: 17041757].
12. Rose AM, Shah AZ, Waseem NH, Chakarova CF, Alfano G, Coussa RG, Ajlan R, Koenekoop RK, Bhattacharya SS. Expression of PRPF31 and TFPT: regulation in health and retinal disease. Hum Mol Genet 2012; 21:4126-37. [PMID: 22723017].
13. Rose AM, Shah AZ, Alfano G, Bujakowska KM, Barker AF, Robertson JL, Rahman S, Sanchez LV, Diaz-Corrales FJ, Chakarova CF, Krishna A, Bhattacharya SS. A Study into the Evolutionary Divergence of the Core Promoter Elements of PRPF31 and TFPT. J Mol Genet Med 2013; 7:1000067-[PMID: 25729402].

14. Sullivan LS, Bowne SJ, Seaman CR, Blanton SH, Lewis RA, Heckenlively JR, Birch DG, Hughbanks-Wheaton D, Daiger SP. Genomic rearrangements of the PRPF31 gene account for 2.5% of autosomal dominant retinitis pigmentosa. Invest Ophthalmol Vis Sci 2006; 47:4579-88. [PMID: 17003455].

15. Yu Y, Rabinowitz R, Steinitz M, Schlesinger M. Correlation between the expression of CD4 and the level of CD4 mRNA in human B-cell lines. Cell Immunol 2002; 215:78-86. [PMID: 12142039].

16. Dausset J, Cann H, Cohen D, Lathrop M, Lalouel JM, White R. Centre d'etude du polymorphisme humain (CEPH): collaborative genetic mapping of the human genome. Genomics 1990; 6:575-7. [PMID: 2184120].

17. Rio Frio T, Civic N, Ransijn A, Beckmann JS, Rivolta C. Two trans-acting eQTLs modulate the penetrance of PRPF31 mutations. Hum Mol Genet 2008; 17:3154-65. [PMID: 18640990].

18. Abu-Safieh L, Vithana EN, Mantel I, Holder GE, Pelosini L, Bird AC, Bhattacharya SS. A large deletion in the adRP gene PRPF31: evidence that haploinsufficiency is the cause of disease. Mol Vis 2006; 12:384-8. [PMID: 16636657].

19. Wang L, Ribaudo M, Zhao K, Yu N, Chen Q, Sun Q, Wang Q. Novel deletion in the pre-mRNA splicing gene PRPF31 causes autosomal dominant retinitis pigmentosa in a large Chinese family. Am J Med Genet A 2003; 121:235-9. [PMID: 12923864].

Articles are provided courtesy of Emory University and the Zhongshan Ophthalmic Center, Sun Yat-sen University, P.R. China. The print version of this article was created on 18 March 2021. This reflects all typographical corrections and errata to the article through that date. Details of any changes may be found in the online version of the article.